# IDEA OF PERFORATED-CORRUGATED WEB PROFILE IN ACHIEVING EFFICIENT STRUCTURAL STEEL SECTION

Hazwani Hasan
*Universiti Sains Malaysia, 14300 Nibong Tebal Penang, Malaysia.*
*Email: wawani127@yahoo.com, Tel: 010-5706092*

Fatimah De'nan
*Universiti Sains Malaysia, 14300 Nibong Tebal Penang, Malaysia.*
*Email: cefatimah@usm.my, Tel: (60)4-5996271*

Choong Kok Keong
*Universiti Sains Malaysia, 14300 Nibong Tebal Penang, Malaysia.*
*Email: cekkc@usm.my, Tel: (60)04-5996225*

**ABSTRACT**

*Triangular web profile (TriWP) steel section with various combinations of perforation shapes, sizes and positions of perforation are investigated under lateral torsional buckling deformation. It involves two stages of analysis by analysing 96 models. The aim of this study is to determine the structural efficiency based on the buckling load, $P_b$. The structural efficiency is determined from the ratio of buckling load to the self-weight. For this purpose, the specimen with three different perforation size between 0.4D to 0.6D, five perforation shapes i.e. circle, square, hexagon, diamond and octagon and three different layouts of perforation, which are Layout 1, Layout 2 and Layout 3 are analysed by using LUSAS 14.3 software to determine the structural efficiency. In Stage 1, the most efficient perforation shape, size and layout of perforation is determined based on the highest structural efficiency value. From the results obtained, the lowest percentage difference of structural efficiency compares to that of the TriWP without perforation is ranged between 2.0% to 18.1%. The TriWP with perforation of diamond in shape and 0.4D in size arranged in Layout 3 shows the highest structural efficiency value i.e. 799.0 produced from the highest buckling load that lead to the most efficient perforation shape, size and layout. Then this type of model is analysed in Stage 2 under different section properties and different span length to observe the performance and its structural behaviour.*

Keywords**:** Perforation web profile, corrugated web profile, finite element analysis, triangular web profile, lateral torsional buckling

## Introduction

In modern building construction, long span beams are commonly used, whereas web openings are only started to be used during the last century in order to reduce the floor depth by passing all services through the web height. The presence of the large openings changes the local transfer of the internal forces, mainly the shear force (Oh et al., 2012). In the last decade, researchers have tried to optimize web opening shapes, sizes and the layout of perforations. This could provide a better understanding of the stress distribution in the vicinity of the web openings, and to examine the structural behaviour under certain types of loading (Tsavdaris and Mello, 2011). The increasing popularity of perforated steel beam is to reduce the cost of materials used, by applying the combination of aesthetic and architectural emphasis in the design consideration of cross-sectional shapes made from standard profiles. The web opening can also be used for cross-passing of utility system in the building floors (Siddh and Pachpor, 2011).

Moreover, corrugated steel webs have recently been proposed to replace the stiffened steel plates of plate girders to improve the aesthetic design of the structure. Corrugated steel plates have been used as building and bridge components due to several advantages such as high shear resistance and out-of-plane stiffness. The usage of corrugated plates as the web I-girders can overcome the disadvantages of conventional stiffened flat webs such as web instability due to bending stress and also provide high fatigue resistance by minimization of the welding process (Moon et al., 2013). The corrugation profile can ensure higher resistibility against shear buckling, leading to the elimination of stiffeners (He et al., 2012). By eliminating the stiffener, hence, the cost of beam fabrication and the weight of structures could be reduced.

## Literature Review

The corrugation profile referred to the shapes of sinusoidal, trapezoidal and semicircular web profiles were found in the literature. The use of corrugated webs is a potential method to achieve adequate out-of-plane stiffness and shear buckling

resistance without using stiffeners: therefore, it considerably reduces the cost of beam fabrication and the weights of superstructure [Korani, 2010].

The investigation on the flexural-torsional buckling strength of an I-girder with corrugated steel webs under linear moment gradient had been done by Moon et al. (2013). It was found that the buckling behaviour of the I-girder with corrugated steel web differed depending on the number of periods of the corrugation. Also, the flange of the girder deformed in the out-of-plane direction with a single curvature and it acts as an internal imperfection when corrugated steel webs have an even number of half corrugation. Moreover, Denan et.al (2010) found that steel beam with trapezoidally corrugated web section have higher resistance to lateral torsional buckling compared to that of section with flat web.

Introducing an opening in the web section of I-beam decreases the critical bending moment that was associated with buckling instability. Serror (2011) found that this decrease depends basically on the ratio (HO/H) between opening height (HO) and beam height (H). A clear increase in the reduction of buckling capacity had been observed when the opening size was kept rising. The layout of the opening also considered as an important matter in this buckling case. It was investigated by Abidin and Izzudin (2013) where the hole near the end support causes a major reduction in beam buckling capacity and results in a lower buckling load factor around the modified region. They had suggested that openings were more suitable to be placed in the low shear zone, particularly in the midspan region. While their use near regions of high shear forces would require the use of stiffeners around the opening to avoid significant reduction in buckling resistance.

**Problem Statement**

The innovation of perforated steel beam from the conventional I-beam has alleviated the cost and material saving in the construction technology. Nevertheless, perforation beams prone to fail under combination of shear and bending. The most dominant failure of the perforated beam with large web opening is vierendeel mechanism. The transfer of shear force across the web openings and the rate of change of the bending moment along the beam are two factors contributing to vierendeel bending (Tsavdaris & Mello, 2012).

In order to overcome this problem, corrugated steel web has recently been used to replace the stiffened steel web of the plate / box girder (Sayed-Ahmed, 2007). Previous studies have proven that the corrugated steel web has better performance compared to the flat web steel section (Abbas et al., 2006; Osman et al., 2007; Moon et al., 2009). Abbas et al. (2006) found that the corrugated-web I-girders have improved shear stability and better fatigue resistance than conventional I-girders with flat webs. In addition, Osman et al. (2007) revealed that TWP section shows a better performance with less deflection as well as stiffer web from buckling. Meanwhile, Moon et al. (2009) discovered that the elastic lateral–torsional buckling strength of the I-girder with corrugated webs increases slightly (maximum 10%) with increasing the corrugation angle, θ compared to that of flat web.

However, in terms of weight, corrugated web beam tends to have greater weight than the flat web because of the corrugation profile. Thus, to improve the usage of the steel beam in the building construction, perforation shapes such as circular, square, hexagonal, octagonal and diamond are proposed in this research. The idea of perforated-corrugated web profile in achieving efficient structural steel section can reduce the weight of the steel section and may achieve similar performance to those without opening.

Furthermore, the structural capacity of TriWP with perforation not yet studied. Hence, the determination of the structural efficiency of TriWP with the combinations of different perforations shapes, sizes and layouts are needed. A three-dimensional finite element model using LUSAS 14.3 is performed to analyse the structural efficiency and structural behaviour of TriWP with perforation subjected to loading conditions such lateral torsional buckling deformation. In addition, the effect of section properties and span length on the structural behaviour and performance of TriWP with perforation need to be observed.

**Model Description**

The model of triangular web profile steel section (TriWP) is developed based on previous researcher (De'nan & Hashim, 2012). In this research, the TriWP with perforation is analysed. Table 1 shows the following section properties of 200 mm × 100 mm × 6 mm × 4 mm which is used to carry out the study in Stage 1. As illustrated in Figure 1, TriWP with perforated web consists of two flanges welded to the triangular profile of the perforated web section.

**Table 1 The dimensional properties of TriWP with and without perforation**

| Depth, $D$ (mm) | Flange width, $B$ (mm) | Flange thickness, $t_f$ (mm) | Web thickness, $t_w$ (mm) | Corrugation angle, θ |
|---|---|---|---|---|
| 200 | 100 | 6 | 4 | 45° |

**Figure 1 Profile of TriWP with perforation**

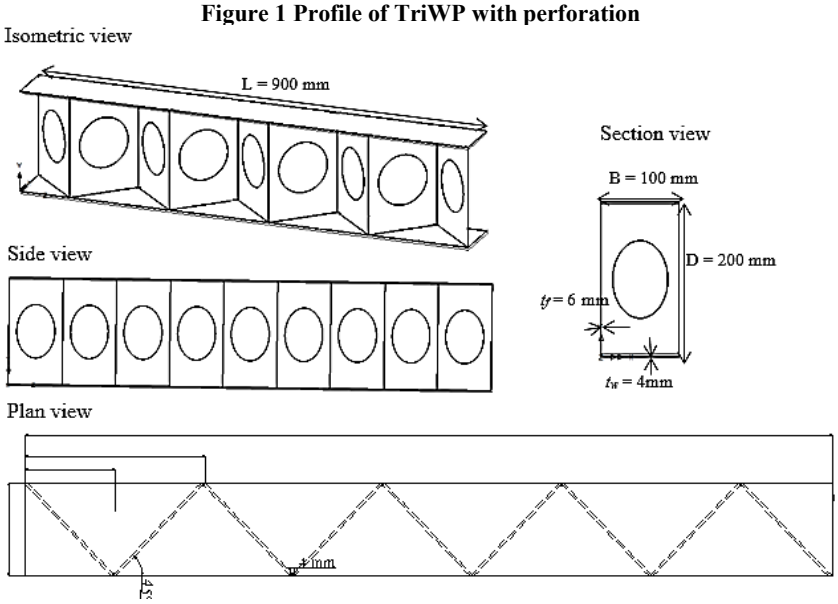


**Perforation Shapes And Sizes**

Perforations in the shape of circle, square, hexagon, diamond and octagon mainly found in the literature (Tsavdaris and Mello, 2012) are proposed in this research as shown in Figure 2. The perforations with the sizes of 0.4D, 0.5D and 0.6D (80 mm, 100 mm, 120 mm) where D is the depth of the section are generated. The perforation shapes as the function of perforation of the web section allows piping system and ducting services to pass through, the sizes of perforation are selected to be between 80 mm to 120 mm.

**Figure 2 TriWP with perforation**

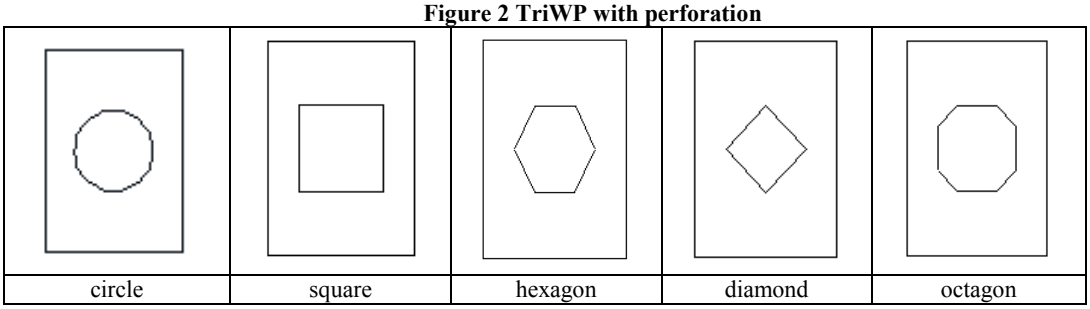

| circle | square | hexagon | diamond | octagon |
|---|---|---|---|---|

**Layouts Of Perforations**

In this study, three different layouts of perforations are used. The arrangement of perforations is located in the middle of the corrugated web section and along the length of the beam. The first layout (Layout 1) locates the perforations along the corrugated web. It begins from the web near both ends of the TriWP. The second layout (Layout 2) and the third layout (Layout 3) locate the perforations in an alternate arrangement. The alternate arrangement for Layout 2 begins from the first end of the corrugated web of the TriWP. Meanwhile, the alternate arrangement for Layout 3 starting from the second end of the corrugated web of the TriWP. The number of perforations depends on the layout of perforations. Layout 1, Layout 2 and Layout 3 consist of 9, 5 and 4 number of perforations respectively. Figure 3 to Figure 5 show examples of the actual views of the respective layout of perforations for circular shape.

**Figure 3 The isometric view of TriWP with perforation of circular shaped arranged in Layout 1**

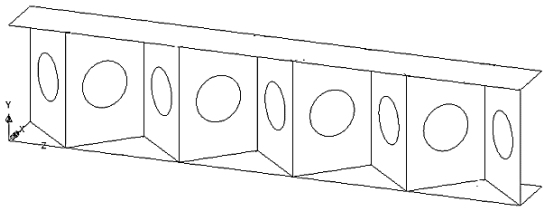

**Figure 4 The isometric view of TriWP with perforation of circular shaped arranged in Layout 2**

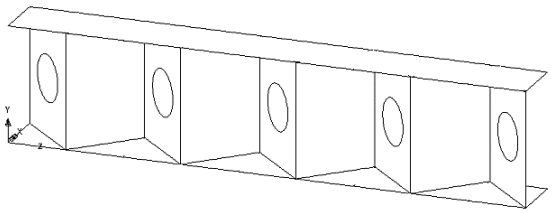

**Figure 5 The isometric view of TriWP with perforation of circular shaped arranged in Layout 3**

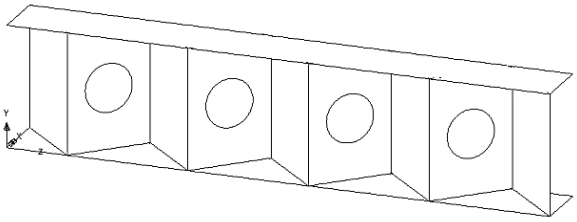

**Methodology**

In Stage 1, the self-weight of TriWP with and without perforation shapes with the dimension of 200 mm × 100 mm × 6 mm × 4 mm and span length of 900 mm is calculated for cases of three different perforation sizes, five different perforation shapes, and three different layouts of perforations. Subsequently, these models have been used in analysis carried out in Stage 1 using finite element method to determine the buckling load, $P_b$ under torsional buckling deformation. Thus, the value of structural efficiency is determined from the ratio of buckling load, $P_b$ to the self-weight. The TriWP with the most efficient perforation shape, size and layout is selected based on structural efficiency determined. In the following step, different web thickness, flange thickness and span length are used on selected models to study the performance and its behaviour. The increasing of load from 0 kN to 120 kN is applied in Stage 1 with the increment of 0 kN, 10 kN, 30 kN, 60 kN, 90 kN and 120 kN. Lastly, 10 kN of the load applied in Stage 2 is used as a constant parameter to observe the behaviour of the model using different section properties and different span length. The detail on each stage is discussed in the next section.

**Finite Element Analysis**

For this research, all the material properties are adopted from the tensile test with Young's Modulus, E, of 226.53 GPa N/mm$^2$, shear modulus, G of 79 x $10^3$ N/mm$^2$ and Poisson ratio of 0.3. These material properties remain constant throughout the analysis. Elastic properties is applied on linear eigenvalue buckling analysis (lateral torsional buckling deformation). Eigenvalue buckling analysis is used by many researchers such as Valdevit et al. (2006); Moon et al. (2009); Umbarkar et al. (2013); Abidin & Izzudin (2013); Saddek (2015) to obtain critical buckling load by solving the associated eigenvalue problems. The load factors are equivalent to the eigenvalue in an eigenvalue buckling analysis. As mentioned by Abidin & Izzudin (2013), the critical buckling load factor ($k_{cr}$) for beams under proportional loading may then be determined directly from the eigenvalue solution. Linear eigenvalue buckling analysis will produce critical loads and buckled shapes. In the lateral torsional buckling resistance, buckling moment resistance is calculated by multiplying the buckling load with the distance of loading from the support.

Thin shell element is used in this study. This is because it is more suitable to structural components which the response is mainly due to flexural or in-plane strains, such as the steel plates making up an I-beam. There are two types of thin shell element, such as quadrilateral thin shell element (QSL8) and triangular thin shell element (TSL6) as shown in Figure 6. In this study, quadrilateral mesh is used and it will generally give better results than a triangular mesh due to the higher-order variation of forces and moments across the elements.

**Figure 6 Triangular thin shell element (TSL6) and Quadrilateral thin shell element (QSL8)**

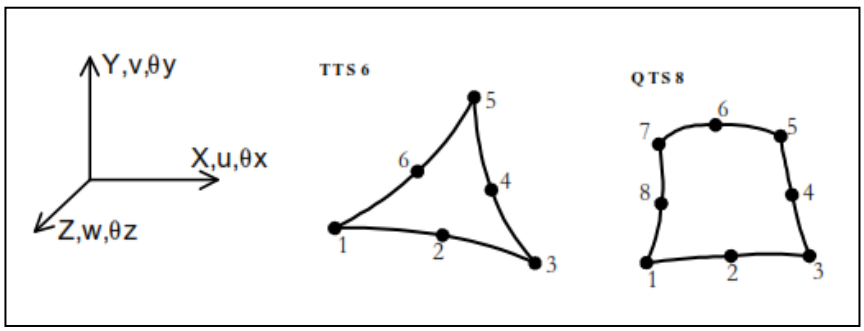


In lateral torsional buckling analysis, the loading and support positions as shown in Figure 7 was adopted from De'nan et al. (2015). The figure shows that the condition of TriWP with perforation after meshing. The symbols of ABCDEFGH are presenting the location of the end nodes of TriWP. On the other hand, the symbol of I is presenting the node in the middle of model length and at the centre of slanting part of the corrugation profile where the loading position is situated. As indicated by De'nan and Hashim (2012), the loading position at the centre of the inclined part gives the minimum deflection among the others loading position. The support position was applied along AB, BC, CD, EF, EG and GH. Both supports are constrained in x, y and z translation direction and fixed at x, y and z rotation. Each support was located at the end of the model by pinned support.

**Figure 7 Supports and loading condition of model for lateral torsional buckling deformation**

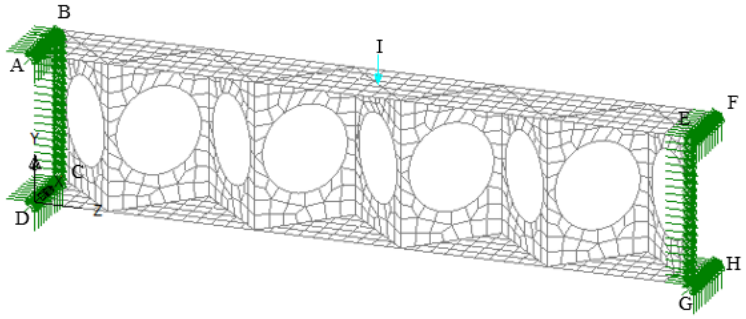


**Determination Of Structural Efficiency**

The structural efficiency in Stage 1 is calculated based on the ratio of buckling load to the self-weight by using Equation 1. The buckling load is generated from eigenvalue buckling analysis. Higher value of buckling load would produce higher structural efficiency. The comparison between TriWP with and without perforation is made by calculating the percentage difference of structural efficiency by using Equation 2.

$$Efficiency = \frac{Buckling\ load\ (kN)}{self-weight\ (kN)} \quad \text{Eq. 1}$$

$$\%\ of\ structural\ efficiency = \frac{c-d}{c} \times 100 \quad \text{Eq. 2}$$

where;
$c$ = structural efficiency of TriWP without perforation
$d$ = structural efficiency of TriWP with perforation

**Result**

**Percentage Weight Reduction**

Table 2 to Table 4 represent the percentage difference of weight reduction of TriWP with and without perforation for Layout 1, Layout 2 and Layout 3, respectively. The presence of perforations such as circular, square, hexagon, octagon and diamond in TriWP reduces the volume of steel usage. Based on the percentage of weight reduction, TriWP with perforation of square shaped shows the highest weight reduction from 0.4D to 0.6D of perforation size for all three layouts of perforations due to the low self-weight compared to another shapes of perforation. The second highest weight reduction is circle which is then followed by hexagon, octagon and diamond. The trend of reduction is significant because it will affect the value of structural efficiency. TriWP with perforation of diamond shaped shows the lowest percentage of weight reduction since it has the highest self-weight. In terms of the layouts of perforations, perforated TriWP with Layout 1 shows the highest percentage of weight reduction ranging from 5.52% to 24.73%. The corresponding percentage values for Layout 2 range from 3.08% to 13.75% and Layout 3 range from 2.47% to 11.01%, respectively. This is because Layout 1 consists of nine numbers of perforations in the web section while Layout 2 and Layout 3 consist of 5 and 4 numbers of perforations, respectively.

**Table 2 Percentage difference of weight reduction of TriWP with perforation for Layout 1**

| **Perforation size** | **Percentage of weight reduction (%)** | | | | |
|---|---|---|---|---|---|
| | TriWP with perforation shape | | | | |
| | Circle | Square | Hexagon | Diamond | Octagon |
| **0.4D** | 8.65 | 11.01 | 8.26 | 5.52 | 7.85 |
| **0.5D** | 13.50 | 17.18 | 12.89 | 8.61 | 12.16 |
| **0.6D** | 19.43 | 24.73 | 18.55 | 12.38 | 17.50 |

**Table 3 Percentage difference of weight reduction of TriWP with perforation for Layout 2**

| **Perforation size** | **Percentage of weight reduction (%)** | | | | |
|---|---|---|---|---|---|
| | TriWP with perforation shape | | | | |
| | Circle | Square | Hexagon | Diamond | Octagon |

| | | | | | |
|---|---|---|---|---|---|
| **0.4D** | 4.82 | 6.13 | 4.61 | 3.08 | 4.35 |
| **0.5D** | 7.51 | 9.56 | 7.18 | 4.80 | 6.77 |
| **0.6D** | 10.81 | 13.75 | 10.32 | 6.89 | 9.74 |

**Table 4 Percentage difference of weight reduction of TriWP with perforation for Layout 3**

| **Perforation size** | **Percentage of weight reduction (%)** | | | | |
|---|---|---|---|---|---|
| | TriWP with perforation shape | | | | |
| | Circle | Square | Hexagon | Diamond | Octagon |
| **0.4D** | 3.86 | 4.91 | 3.69 | 2.47 | 3.48 |
| **0.5D** | 6.02 | 7.66 | 5.75 | 3.84 | 5.42 |
| **0.6D** | 8.65 | 11.01 | 8.26 | 5.52 | 7.79 |

In Stage 1, analysis involving 46 models are developed under lateral torsional buckling deformation to determine the buckling load. Table 5 shows the analysis result of buckling load, $P_b$, of TriWP with perforation for Layout 1, Layout 2 and Layout 3. The results indicate that increasing the perforation area of each perforation shape and layout would lead to reduction in the buckling load. Among the layouts of perforations, case of Layout 3 shows the highest buckling load compared to others layout. Smaller perforation size results in higher buckling load. In this case, TriWP with perforation of diamond in shape and 0.4D in size arranged in Layout 3 shows the highest buckling load i.e. 125.92 kN. While calculating the buckling load, $P_b$, the value of buckling moment resistance, $M_{b,Rd}$, is also calculated to determine the resistance of the beams towards buckling as shown in Table 6.

It is found that TriWP with perforation for Layout 3 shows the highest buckling moment resistance value among all perforation shapes. The highest buckling moment resistance of 56.67 kNm is found in the case of TriWP with perforation of diamond in shape and 0.4D in size. TriWP with perforation of square in shape shows the lowest moment buckling resistance for all perforation sizes and layouts. This is because the geometry of square shape has bigger perforation area compared to other shapes which affects the moment buckling resistance. The typical result of the of displacement contour is shown in Figure 8 for the case of TriWP with perforation size of 0.4D under lateral torsional buckling for Layout 1, Layout 2 and Layout 3.

**Table 5 The Buckling load of TriWP with perforation**

| **Perforation shape** | **Buckling load, $P_b$ (kN)** | | | | | | | | |
|---|---|---|---|---|---|---|---|---|---|
| | **Layout 1** | | | **Layout 2** | | | **Layout 3** | | |
| | **0.4D** | **0.5D** | **0.6D** | **0.4D** | **0.5D** | **0.6D** | **0.4D** | **0.5D** | **0.6D** |
| **Circle** | 97.75 | 91.87 | 86.02 | 97.74 | 91.77 | 86.60 | 122.42 | 107.54 | 101.80 |
| **Square** | 92.88 | 84.14 | 73.78 | 92.78 | 82.68 | 75.50 | 105.65 | 105.90 | 105.38 |
| **Hexagon** | 97.72 | 91.87 | 84.88 | 115.03 | 91.69 | 85.32 | 105.41 | 105.30 | 105.11 |
| **Diamond** | 100.66 | 97.41 | 110.32 | 118.46 | 114.77 | 93.96 | 125.92 | 121.17 | 109.18 |
| **Octagon** | 96.37 | 89.70 | 82.34 | 96.44 | 89.69 | 82.76 | 105.49 | 105.22 | 105.78 |

**Table 6 Moment buckling resistance of TriWP with perforation**

| **Perforation shape** | **Buckling moment resistance, $M_{b,Rd}$ (kNm)** | | | | | | | | |
|---|---|---|---|---|---|---|---|---|---|
| | **Layout 1** | | | **Layout 2** | | | **Layout 3** | | |
| | **0.4D** | **0.5D** | **0.6D** | **0.4D** | **0.5D** | **0.6D** | **0.4D** | **0.5D** | **0.6D** |
| **Circle** | 43.99 | 41.34 | 38.71 | 43.98 | 41.30 | 38.97 | 55.09 | 54.53 | 45.81 |
| **Square** | 41.80 | 37.86 | 33.20 | 41.75 | 37.21 | 33.97 | 47.54 | 47.66 | 47.42 |
| **Hexagon** | 43.98 | 41.34 | 38.20 | 51.76 | 41.26 | 38.40 | 47.43 | 47.39 | 47.30 |
| **Diamond** | 45.30 | 43.84 | 49.64 | 53.31 | 51.65 | 42.28 | 56.67 | 48.39 | 49.13 |
| **Octagon** | 43.37 | 40.37 | 37.05 | 43.40 | 40.36 | 37.24 | 47.47 | 47.35 | 47.60 |

**Figure 8 The displacement contour for TriWP with perforation of diamond in shape and 0.4D in size under lateral torsional buckling deformation (10 kN)**

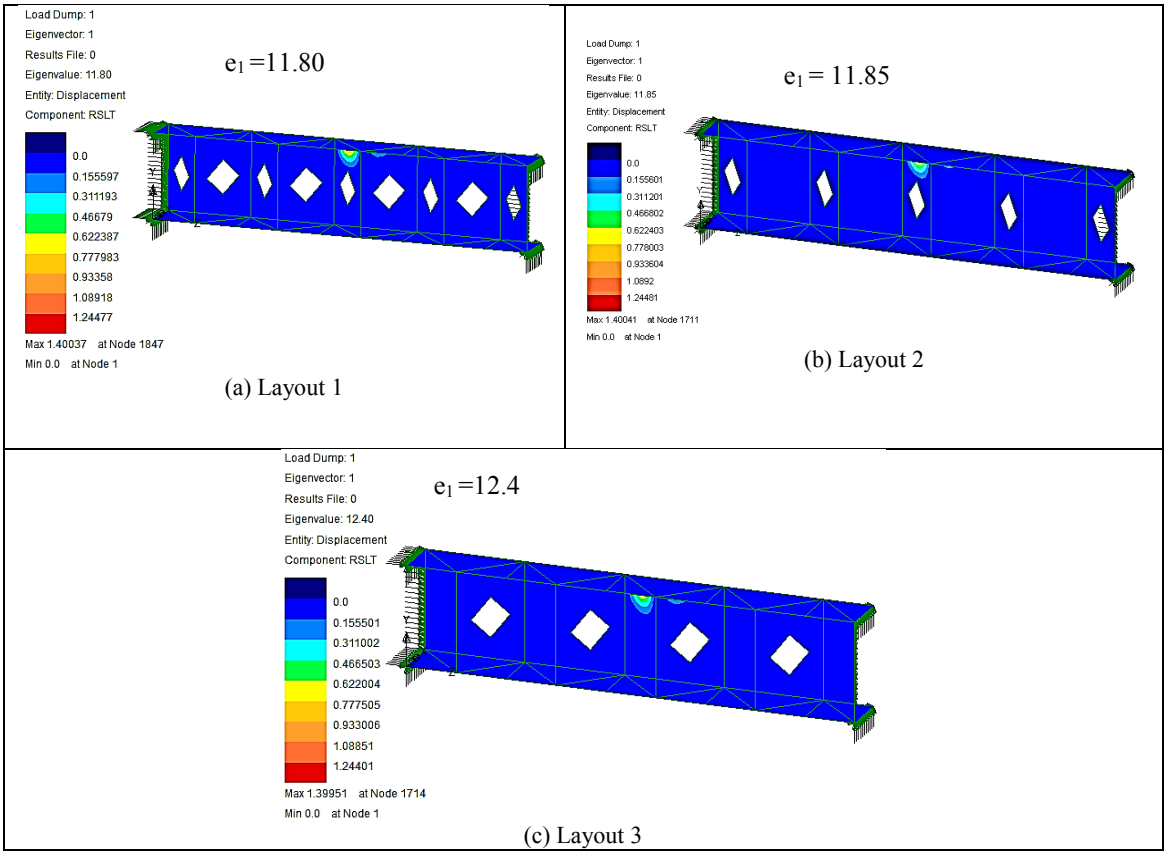


The results obtained are then compared with previous studies. It is expected that introducing an opening in the web section of I-beam decreases the critical bending moment. As stated in the literature review section, a clear increase in the reduction of buckling capacity is observed when the opening size is increased. The layouts of the opening also considered as an important matter which affects the buckling capacity as mentioned by Abidin and Izzudin (2013). For that reason, in this research study, model with Layout 3 shows the highest buckling moment resistance for all perforation shapes because the location of perforation is near the mid-span of beam section. However, both previous study (Serror (2011); Abidin and Izzudin (2013)) are focused on the steel I-beam with various web opening. But, the contribution of this research finding is focused on the corrugated steel section i.e. TriWP with perforation.

The values of structural efficiency of all models are summarized in Table 7. The highest of structural efficiency i.e. 799.0 is produced from the highest buckling load shown in TriWP with perforation of diamond in shape and 0.4D in size arranged in Layout 3. The results of percentage difference (Eq.2) are then presented to compare the value of structural efficiency of TriWP with and without perforation as indicated in Table 8. The range of percentage for all perforation shapes and sizes are 4.4% to 25.6%, 7.2% to 33.6% and 2.0% to 18.1% for Layout 1, Layout 2 and Layout 3, respectively. This means Layout 3 shows the lowest percentage difference of structural efficiency and diamond at perforation size of 0.4D has the lowest percentage difference i.e. 2.0%. It shows that this model has high structural efficiency compared to the others and its value is very close to TriWP without perforation. Due to the above reason, TriWP with perforation of diamond in shape and 0.4D in size arranged in Layout 3 is selected for further analysis in the Stage 2 under lateral torsional buckling deformation.

**Table 7 Structural efficiency of TriWP with perforation**

| Perforation shape | Structural efficiency | | | | | | | | |
|---|---|---|---|---|---|---|---|---|---|
| | Layout 1 | | | Layout 2 | | | Layout 3 | | |
| | 0.4D | 0.5D | 0.6D | 0.4D | 0.5D | 0.6D | 0.4D | 0.5D | 0.6D |
| **Circle** | 662.3 | 657.1 | 660.7 | 635.5 | 614.3 | 600.9 | 788.3 | 797.7 | 689.7 |
| **Square** | 645.9 | 628.8 | 606.7 | 615.0 | 565.9 | 541.6 | 687.4 | 709.8 | 732.8 |
| **Hexagon** | 659.4 | 652.5 | 645.0 | 746.4 | 611.3 | 588.8 | 677.4 | 691.4 | 709.2 |

| | | | | | | | | | |
|---|---|---|---|---|---|---|---|---|---|
| **Diamond** | 659.2 | 659.5 | 779.1 | 756.5 | 746.2 | 624.3 | 799.0 | 692.0 | 715.0 |
| **Octagon** | 647.2 | 632.0 | 617.7 | 623.8 | 595.6 | 567.2 | 676.2 | 688.6 | 667.8 |

**Table 8 The percentage difference of structural efficiency**

| Perforation shape | Percentage difference of structural efficiency (%) | | | | | | | | |
|---|---|---|---|---|---|---|---|---|---|
| | Layout 1 | | | Layout 2 | | | Layout 3 | | |
| | 0.4D | 0.5D | 0.6D | 0.4D | 0.5D | 0.6D | 0.4D | 0.5D | 0.6D |
| **Circle** | 18.8 | 19.4 | 19.0 | 22.1 | 24.7 | 26.3 | 3.3 | 13.2 | 15.4 |
| **Square** | 20.8 | 22.9 | 25.6 | 24.6 | 30.6 | 33.6 | 15.7 | 12.9 | 10.1 |
| **Hexagon** | 19.1 | 20.0 | 20.9 | 8.5 | 25.0 | 27.8 | 16.9 | 15.2 | 13.0 |
| **Diamond** | 19.1 | 19.1 | 4.4 | 7.2 | 8.5 | 23.4 | 2.0 | 4.4 | 12.3 |
| **Octagon** | 20.6 | 22.5 | 24.2 | 23.5 | 27.0 | 30.4 | 17.1 | 15.5 | 18.1 |

**Parametric Study**

Section properties have a great effect on the behaviour of beam under lateral torsional buckling deformation. Effect of web thickness ($t_w$) and flange thickness ($t_f$) are the main focus in Stage 2 by using different span length ($L$). A total of 50 finite element models are analysed under this parametric study to observe the structural performance and buckling moment resistance, $M_{b,Rd}$.

In this section, a parametric study is carried out to investigate the influence of the section properties and span length on the performance and structural behaviour of TriWP with perforation. The model is designed based on the previous stage of numerical analysis where the selected model is chosen based on the structural efficiency i.e. TriWP with perforation of diamond in shape and 0.4D in size arranged in Layout 3. The selected model is analysed for different section properties and different span length. By fixing the depth of the section (D), flange width (B) and the corrugation angle (θ), the models are designed with different web thickness, flange thickness and span length. The constant load applied about 10 kN is used to observe the effect of different section properties. 10 kN is used as reference load and it is suitable to use since it doesn't exceed the load at yield.

**Effect Of Web Thickness, $t_w$**

Each model of TriWP steel section with perforation as shown in Table 9 is designed for different span length from 1 m to 5 m. These 25 models are used to study the influence of web thickness on the structural behaviour under increasing length of the section. Other geometric parameters are kept constant i.e. D = 200 mm, B = 100 mm, θ = 45° and $t_f$ = 8 mm. The following web thicknesses are considered; $t_w$ = 2 mm, 4 mm, 5 mm, 6 mm and 7 mm.

**Table 9 Model with different web thickness**

| Section | Depth, $D$ (mm) | Flange width, $B$ (mm) | Flange thickness, $t_f$ (mm) | Web thickness, $t_w$ (mm) |
|---|---|---|---|---|
| 200 × 100 × 8 × 2 | 200 | 100 | 8 | 2 |
| 200 × 100 × 8 × 4 | 200 | 100 | 8 | 4 |
| 200 × 100 × 8 × 5 | 200 | 100 | 8 | 5 |
| 200 × 100 × 8 × 6 | 200 | 100 | 8 | 6 |
| 200 × 100 × 8 × 6 | 200 | 100 | 8 | 7 |

**Effect Of Flange Thickness, $t_f$**

Each model of TriWP steel section with perforation as shown in Table 10 is designed for different span length from 1 m to 5 m. These 25 models are used to study the influence of flange thickness on the structural behaviour under increasing length of the section. Other geometric parameters are kept constant at D = 200 mm, B = 100 mm, θ = 45° and $t_w$ = 3 mm. The following web thicknesses are considered; $t_f$ = 4 mm, 5 mm, 6 mm, 7 mm and 8 mm.

**Table 10 Model with different flange thickness**

| Section | Depth, $D$ (mm) | Flange width, $B$ (mm) | Flange thickness, $t_f$ (mm) | Web thickness, $t_w$ (mm) |
|---|---|---|---|---|
| 200 × 100 × 4 × 3 | 200 | 100 | 4 | 3 |
| 200 × 100 × 5 × 3 | 200 | 100 | 5 | 3 |
| 200 × 100 × 6 × 3 | 200 | 100 | 6 | 3 |
| 200 × 100 × 7 × 3 | 200 | 100 | 7 | 3 |
| 200 × 100 × 8 × 3 | 200 | 100 | 8 | 3 |

The structural performance and buckling moment resistance, $M_{b,Rd}$ are affected by flange thickness, web thickness, and span length. The buckling moment resistance obtained from eigenvalue analysis of selected model with different flange and web thickness and span length is presented in the following figures. As expected, when the length of the model increases, the buckling moment resistance decreases. Under the same web thickness, the buckling moment resistance is found to increase when the flange thickness is increased as shown in Figure 9. Meanwhile, under the same flange thickness, the buckling moment resistance is found to increase with increase in the web thickness as shown in Figure 10. Both sets of the result show similar trend. By increasing the flange and web thickness, the buckling moment resistance increases under the same span length. The larger thickness of the web or flange are significantly affect to the buckling moment resistance where the models have more resistance to buckle. Also, increase the span length would lead the reduction of buckling moment resistance.

**Figure 9 $M_{b,Rd}$ versus flange thickness for TriWP with perforation of diamond in shape and 0.4D in size arranged in Layout 3**

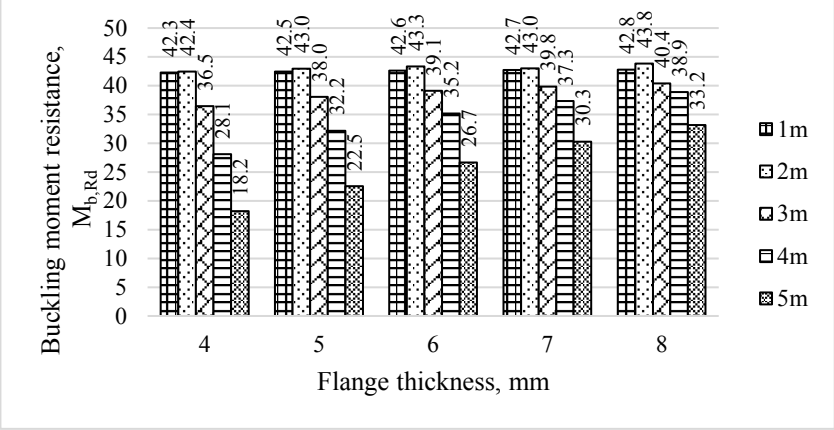


**Figure 10 $M_{b,Rd}$ versus web thickness for TriWP with perforation of diamond in shape and 0.4D in size arranged in Layout 3**

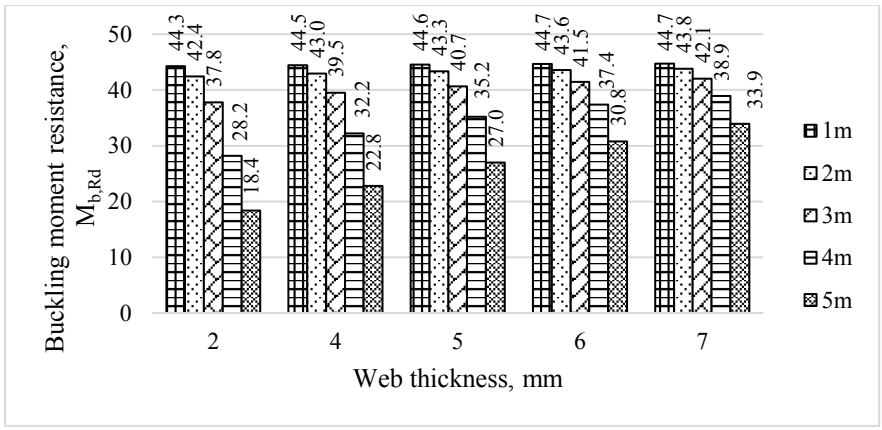

**Conclusion**

Nine-ty six models of TriWP with and without perforation have been studied. The self-weight of the models was first determined. They were analysed using finite element analysis to investigate lateral torsional deformation. Load carrying capacity were investigated to determine the structural efficiency. The following conclusion can be drawn from the present study:

**a)** For each perforation shape and the layout, the percentage of weight reduction is found to increase as the perforation size increases. Thus, the value of structural efficiency also increases. In Stage 1 of the study, the TriWP with the perforation of diamond in shape and 0.4D in size arranged in Layout 3 showed the highest buckling moment resistance lateral torsional buckling deformation. Therefore, it contributes to the highest value of structural efficiency (799.0) and leads to the most efficient perforation shape, size and layout. Good agreement can be observed between the result of finite element analysis and previous studies found in the literature. Compared to other researchers, the contribution of the analysis of this study is the structural efficiency of TriWP with perforation. The result of analysis is used to determine the structural efficiency of each model.

b) In Stage 2 of study, it is found that when the web and flange thickness are increased under the same span length with constant flange and web depth, the value of moment buckling resistance also increased under loading causing lateral torsional buckling. Meanwhile, increase in span length of model results in lower moment buckling resistance.

**ACKNOWLEDGMENT**
The authors would like to express their deepest appreciation to the financial support of Universiti Sains Malaysia grant under FRGS (Account Number: 203/PAWAM/6071239) in funding this project.

**References**

Abidin, A. R.Z., & Izzuddin, B. A. (2013). Meshless local buckling analysis of steel beams with irregular web openings. *Engineering Structures*, *50*, 197–206.

Bower, J.E., Design of beams with web openings. Journal of structural division.

Brando, G., & De Matteis, G. (2013). Buckling resistance of perforation steel angle members. *Journal of Constructional Steel Research*, *81*, 52–61.

Denan, F., & Hashim, N. S. (2012). The Effect of Web Corrugation Angle on Bending Performance of Triangular Web Profile Steel Beam Section. *International Journal of Energy Engineering*, *2*(1), 1–4.

De'nan.F, M. . (2015). The Effect of web Opening On Lateral Torsional Behaviour of Triangular Web Profile Steel Beam Section. *Proceeding of International Conference on Science, Technology & Social Science*, (December).

Denan, F., Osman, M. H., Saad, S., & Campus, E. (2010). The Study of Lateral Torsional Buckling Behaviour Of Beam With Trapezoid Web Steel Section By Experimental. *International Journal of Research and Reviews in Applied Science*, *2*(March), 232–240.

Hasan, H., De, F., & Keong, C. K. (2015). Experimental Study on Lateral -Torsional Buckling of Triangular Web Profile Steel Section. *Applied Mechanic and Materials*, *802*, 178–183.

Korani,N.,K., H. R. (2010). Lateral bracing of I-girder with corrugated webs under uniform bending. *Journal of Constructional Steel Research*, *66*(12), 1502–1509.

Moon, J., Lim, N.-H., & Lee, H.-E. (2013). Moment gradient correction factor and inelastic flexural–torsional buckling of I-girder with corrugated steel webs. *Thin-Walled Structures*, *62*, 18–27.

Moon, J., Yi, J.-W., Choi, B. H., & Lee, H.-E. (2009). Lateral–torsional buckling of I-girder with corrugated webs under uniform bending. *Thin-Walled Structures*, *47*(1), 21–30.

Saddek, A. B. (2015). Theoretical Investigation of Shear Buckling for Hybrid Steel Plate Girder with Corrugated Webs. *World Applied Sciences Journal*, 2, p. 284-302

Serror, M. H. (2011). Effect of Web Opening on Buckling Instability of Simply Supported Steel I-Beam. *Journal of Civil Engineering and Architechture*, *5*(9), 809–818.

Sweedan, A. M. I., & El-Sawy, K. M. (2011). Elastic local buckling of perforation webs of steel cellular beam column elements. *Journal of Constructional Steel Research*, *67*(7), 1115–1127.

Tsavdaridis, K. D., & D'Mello, C. (2012). Optimisation of novel elliptically-based web opening shapes of perforation steel beams. *Journal of Constructional Steel Research*, *76*, 39–53.

Tsavdaridis, K. D., & D'Mello, C. (2011). Web buckling study of the behaviour and strength of perforation steel beams with different novel web opening shapes. *Journal of Constructional Steel Research*, *67*(10), 1605–1620.

Umbarkar, K. R., Patton, L. M., & Singh, K. D. (2013). Effect of single circular perforation in lean duplex stainless steel (LDSS) hollow circular stub columns under pure axial compression. *Thin-Walled Structures*, *68*, 18–25.

Valdevit, L., Wei, Z., Mercer, C., Zok, F. W., & Evans, a. G. (2006). Structural performance of near-optimal sandwich panels with corrugated cores. *International Journal of Solids and Structures*, *43*(16), 4888–4905.